Supplementary Information

GGTase-I deficiency hyperactivates macrophages and induces erosive arthritis in mice

Omar M. Khan, Mohamed X. Ibrahim, Ing-Marie Jonsson, Christin Karlsson, Meng Liu, Anna-Karin M. Sjogren, Frida J. Olofsson, Mikael Brisslert, Sofia Andersson, Claes Ohlsson, Lillemor Mattsson Hultén, Maria Bokarewa, and Martin O. Bergo

SUPPLEMENTARY METHODS

Computerized Tomography

Peripheral quantitative computerized tomography (PQCT) scans were performed *ex vivo* on the tibia with a PQCT XCT RESEARCH M (version 4.5B; Norland), operating at a resolution of 70 μm as described (1). For quantification of trabecular bone mineral density (BMD), the scan was performed in the metaphyseal part of the proximal tibia; for cortical bone parameters, the scan was performed in the mid-diaphyseal region. Micro-CT analyses were performed on the distal femur with a Skyscan 1072 scanner (SkyScan) and imaged with an X-ray tube (100 kV, 98 μA). The scanning angular rotation was 180°, the angular increment was 0.90°, and the isotropic volume-pixel size was 6.51 μm. Images were generated by reconstructing datasets with a modified Feldkamp algorithm and segmenting them into binary images by adaptive local thresholding.

T lymphocyte–dependent and –independent immune responses in vivo

T lymphocyte–independent inflammation was induced by injecting 30 μl of olive oil in a hind paw which primarily recruits neutrophils. The thickness of the paw was measured before and 24 h after the injection (2). T lymphocyte–dependent inflammation was evaluated with the delayed-type hypersensitivity reaction induced by 4-ethoxymethylene-2-phenyloxazolone as described (2).

Immunocytochemistry

Differentiated BM macrophages were plated in 8-well chamber slides (10^4 cells/well). The cells were incubated with 10 μM GGTI-298 (Sigma, G5169) and 5 μM FTI (Lonafarnib, Schering-Plough) for 16 h. Cells were fixed in methanol and incubated with antibodies recognizing RAC1 (ARC03) as described in Methods and prelamin A as described (3).

SUPPLEMENTARY REFERENCES

1. Windahl, SH, Vidal, O, Andersson, G, Gustafsson, JA, and Ohlsson, C. Increased cortical bone mineral content but exchanged trabecular bone mineral density in female ER beta(-/-) mice. *J. Clin. Invest.* 1999;104:895–901.
2. Verdrengh, M, Jonsson, IM, Holmdahl, R, and Tarkowski, A. Genistein as an anti-inflammatory agent. *Inflamm. Res.* 2003;52:341–346.
3. Liu, M, et al. Targeting the protein prenyltransferases efficiently reduces tumor development in mice with K-RAS-induced lung cancer. *Proc. Natl. Acad. Sci. U S A* 2010;107:6471–6476.

SUPPLEMENTARY FIGURE LEGENDS

Supplementary Figure 1 (**A**) Micro-CT scans of the distal femur showing the articular surface of the knee joint of a *Pggt1b$^{fl/+}$LC* and a *Pggt1b$^{fl/fl}$LC* mouse. Arrows indicate site of erosion. (**B,C,D**) PQCT scanning was used to quantify trabecular bone mineral density (BMD) (**B**), cortical BMD (**C**), and cortical thickness (**D**) in the tibia of 12-week-old *Pggt1b$^{fl/+}$LC* and *Pggt1b$^{fl/fl}$LC* mice (*n* = 10/genotype). (**E**) Hematoxylin and eosin–stained sections of tissues from 12-week-old *Pggt1b$^{fl/+}$LC* and *Pggt1b$^{fl/fl}$LC* mice. Similar histology was seen in four additional mice/genotype. Scale bar, 400 μm. (**F**) Immunohistochemical staining of lung and bone marrow sections of 12-week-old mice to document the specificity of the non-prenylated (np)-RAP1A antibody. Note the absence of staining in tissues from a control *Pggt1b$^{fl/+}$LC* mouse. Scale bar, 35 μm. (**G**) Neutrophil infiltration measured as an increase in paw thickness of mice injected subcutaneously with olive oil (*n* = 5/genotype). (**H**) T lymphocyte–dependent inflammation measured as an increase in ear thickness after an oxa-mediated delayed-type hypersensitivity reaction (*n* = 5/genotype). Data are expressed as mean ± SEM.

Supplementary Figure 2 (**A**) Hematoxylin and eosin–stained sections of joints from wild-type (8 weeks old at transplant) and *Pggt1b$^{fl/fl}$LC* (12 weeks old at transplant) mice that were lethally irradiated and transplanted with *Pggt1b$^{fl/fl}$LC* and wild-type

BM, respectively. The mice were killed 14 weeks after transplantation. E, erosion; S, synovium. Scale bar, 200 μm (**B**) Synovitis and bone erosion evaluated in knee, ankle, metatarsal, elbow, wrist, and metacarpal joints of wild-type (8 weeks old at transplant) and *Pggt1b*$^{fl/fl}$*LC* (12 weeks old at transplant) mice transplanted with wild-type and *Pggt1b*$^{fl/fl}$*LC* BM, respectively (*n* = 4/genotype). The mice were killed 14 weeks after transplantation. Data are expressed as mean ± SEM.

Supplementary Figure 3 (**A**) Western blots illustrating the reduced electrophoretic mobility of affinity purified RAC1 in extracts of *Pggt1b*$^{fl/fl}$*LC* compared to *Pggt1b*$^{fl/+}$*LC* BM macrophages in multiple experiments. Protein extracts were resolved on 10% or 12% Tris-HCl Protean gels with the 20 kDa molecular weight marker run to the lower end of the gel. (**B)** Western blot illustrating the reduced migration of affinity purified RAC1 in extracts of *Pggt1b*$^{fl/fl}$*LC* BM macrophages and *Pggt1b*$^{fl/+}$*LC* BM macrophages incubated with 10 μM GGTI for 24 h. (**C**) Western blots of lysates from *Rac1*$^{fl/fl}$ mouse embryonic fibroblasts incubated with adenoviruses expressing Cre (to produce *Rac1* null cells) or β-gal (to produce control parental cells) to document the specificity of the RAC1 antibodies from Millipore (used in Figure 3D, 3F and 3G) and Pierce (used in Figure 3A and Supplementary Figure 3A). (**D**) Confocal micrographs documenting the specificity of the RAC1 antibody used for immunocytochemistry (ARC03, Cytoskeleton) in Figure 3E and Supplementary Figure 3D. Note reduced immunofluorescence of RAC1 in cells incubated for 3 d with a *RAC1*-shRNA lentivirus compared to control *RAC2*-shRNA lentivirus. Scale bar, 100 μm. (**E**) Confocal micrographs showing immunofluorescence staining of RAC1 and prelamin A in *Pggt1b*$^{fl/fl}$*LC* and *Pggt1b*$^{fl/+}$*LC* BM macrophages incubated with 5 μM FTI and 10 μM GGTI for 24 h. Evidence that the GGTI was inhibiting GGTase-I is illustrated by the reduced cell adhesive area of the *Pggt1b*$^{fl/+}$*LC* cells. Evidence that the FTI was inhibiting FTase is illustrated by the prelamin A staining (prelamin A is normally farnesylated by FTase and rapidly processed to mature lamin A; when FTase is inhibited, nonfarnesylated prelamin A accumulates and is detected by the antibody). Scale bars, 10 μm.

Supplementary Figure 4 (**A**) RT-QPCR analyses confirming the increased expression of the indicated genes in LPS-stimulated *Pggt1b*$^{fl/fl}$*LC* compared to *Pggt1b*$^{fl/+}$*LC* BM macrophages (*n* = 3/genotype). The primers were different from those used in Figures 4E and F. (**B**) RT-QPCR analyses showing relative expression of the genes in **A** using cDNA from LPS-stimulated *Pggt1b*$^{fl/fl}$*LC* and *Pggt1b*$^{fl/+}$*LC* intraperitoneal (IP) macrophages. Data are expressed as the mean (*n* = 3/genotype).

Supplementary Figure 1

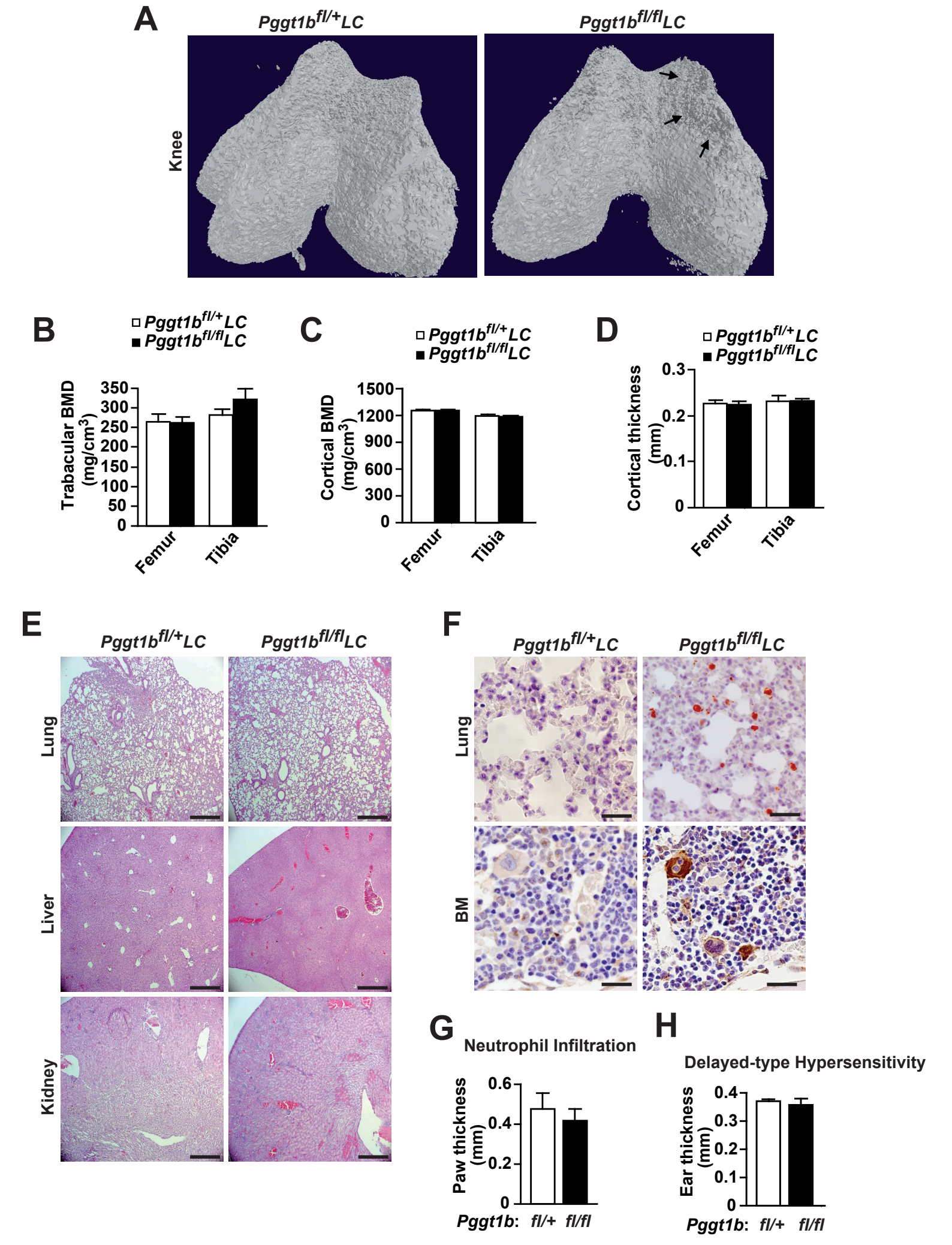

Supplementary Figure 2

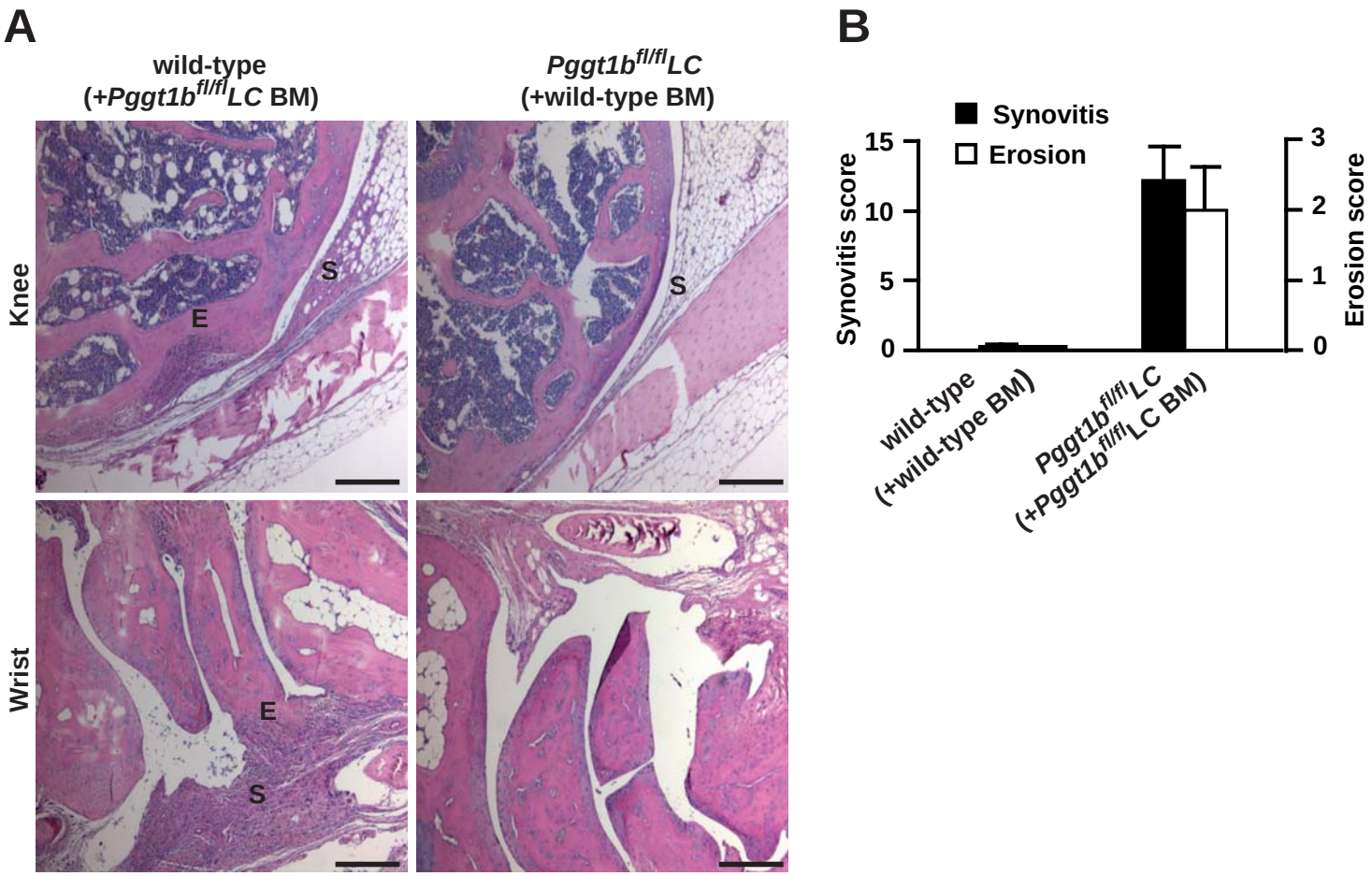

Supplementary Figure 3

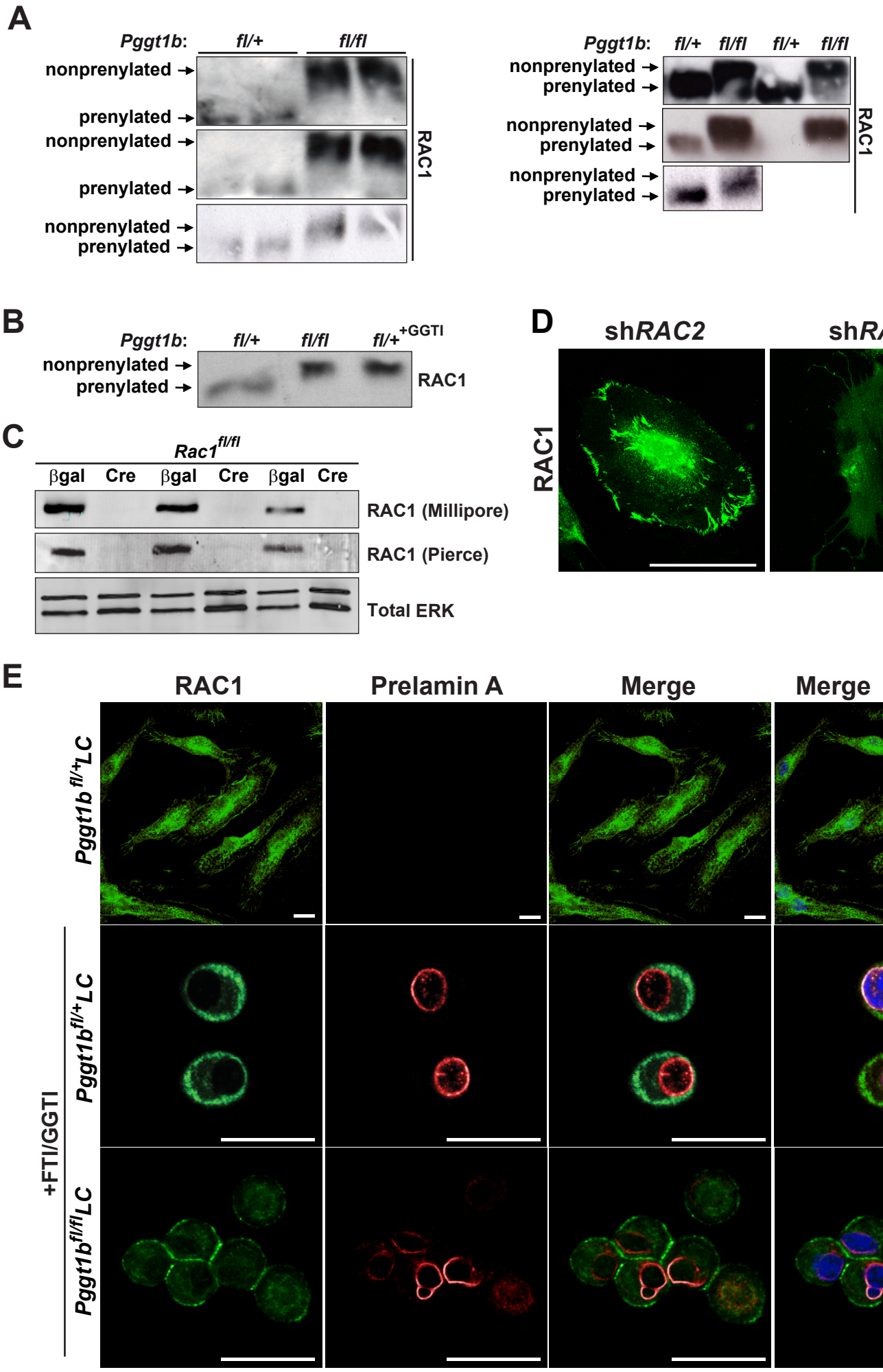

Supplementary Figure 4

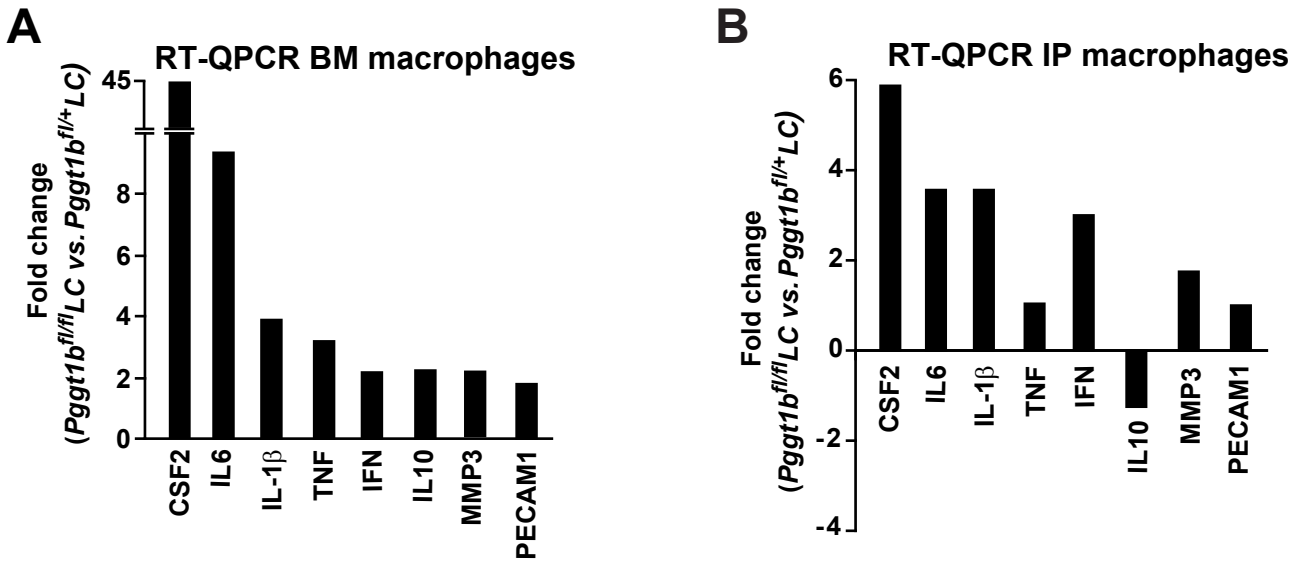

Supplementary Table 1

Mouse NFκB Signaling Pathway PCR Array
(*Pggt1b$^{fl/fl}$LC vs Pggt1b$^{fl/+}$LC*)

Gene	Fold change	p value
Akt1	1.28	0.435
Atf1	1.40	0.196
Atf2	2.15	0.112
Bcl10	1.59	0.292
Bcl3	2.27	0.060
C3	1.31	0.521
Card10	1.95	0.121
Nod1	1.40	0.486
Casp1	1.11	0.764
Casp8	1.37	0.473
Ccl2	2.74	0.072
Cflar	2.42	0.113
Chuk	1.64	0.154
Crebbp	1.53	0.150
Csf2	44.75	0.00001
Csf3	15.82	0.00006
Edg2	1.66	0.176
Egr1	2.05	0.144
Elk1	0.98	0.957
F2r	2.91	0.012
Fadd	1.14	0.815
Fasl	1.64	0.246
Fos	0.71	0.525
Gja1	4.26	0.012
Htr2b	1.07	0.892
Icam1	1.27	0.509
Ifng	2.87	0.058
Ikbkb	1.61	0.190
Ikbke	1.01	0.971
Ikbkg	1.82	0.232
Il10	2.39	0.123
Il1a	5.31	0.002
Il1b	5.73	0.001
Il1r1	1.09	0.867
Il6	8.06	0.001
Irak1	1.06	0.902
Irak2	1.70	0.134
Irf1	1.18	0.524
Jun	1.13	0.629
Lta	2.83	0.007
Ltbr	1.09	0.793
Map3k1	0.93	0.882
Mapk3	1.01	0.991
Myd88	1.06	0.901
Nlrp12	2.04	0.109

Gene	Fold change	p value
Nfkb1	1.73	0.254
Nfkb2	1.17	0.686
Nfkbia	1.31	0.556
Pcaf	1.34	0.227
Eif2ak2	0.95	0.816
Raf1	1.63	0.035
Rel	2.06	0.031
Rela	1.22	0.481
Relb	1.20	0.614
Ripk1	1.17	0.702
Ripk2	1.48	0.408
Slc20a1	1.24	0.576
Smad3	0.64	0.365
Stat1	0.84	0.638
Tbk1	1.46	0.270
Tgfbr1	0.71	0.312
Tgfbr2	0.50	0.007
Tlr1	1.29	0.304
Tlr2	0.89	0.619
Tlr3	0.49	0.010
Tlr4	1.70	0.154
Tlr6	1.34	0.442
Tlr7	1.04	0.935
Tlr8	0.56	0.153
Tlr9	0.50	0.136
Tnf	4.00	0.010
Tnfaip3	2.98	0.043
Tnfrsf10b	1.04	0.876
Tnfrsf1a	1.07	0.615
Tnfrsf1b	1.21	0.459
Cd40	1.65	0.179
Cd27	1.98	0.174
Tnfsf10	0.41	0.001
Tnfsf14	0.97	0.906
Tollip	1.19	0.610
Tradd	1.10	0.710
Traf2	0.80	0.491
Traf3	1.17	0.650
Zap70	2.03	0.194
Gusb	0.96	0.841
Hprt1	0.69	0.585
Hsp90ab1	1.54	0.046
Gapdh	1.09	0.669
Actb	0.90	0.585

Supplementary Table 2

Mouse Extracellular Matrix and Adhesion Molecules PCR Array
(*Pggt1b$^{fl/fl}$LC vs Pggt1b$^{fl/+}$LC*)

Gene	Fold change	p value
Adamts1	4.45	0.025
Adamts2	4.04	0.184
Adamts5	2.27	0.194
Adamts8	1.94	0.275
Ctnna1	2.30	0.170
Ctnna2	1.85	0.266
Ctnnb1	1.59	0.446
Cd44	3.40	0.062
Cdh1	1.32	0.698
Cdh2	4.84	0.106
Cdh3	1.81	0.288
Cdh4	2.60	0.293
Cntn1	1.96	0.225
Col1a1	1.66	0.699
Col2a1	2.60	0.207
Col3a1	5.88	0.101
Col4a1	2.12	0.175
Col4a2	1.84	0.179
Col4a3	1.52	0.544
Col5a1	3.17	0.240
Col6a1	3.41	0.196
Vcan	2.98	0.080
Ctgf	2.98	0.463
Ecm1	2.40	0.062
Emilin1	1.02	0.964
Entpd1	1.00	0.994
Fbln1	1.67	0.549
Fn1	81.06	0.002
Hapln1	1.81	0.289
Hc	1.84	0.063
Icam1	1.98	0.201
Itga2	3.31	0.148
Itga3	2.72	0.180
Itga4	1.63	0.273
Itga5	1.87	0.160
Itgae	1.63	0.478
Itgal	1.85	0.323
Itgam	1.81	0.253
Itgav	1.58	0.443
Itgax	1.26	0.761
Itgb1	1.64	0.294
Itgb2	2.31	0.048
Itgb3	1.75	0.382
Itgb4	1.31	0.674
Lama1	1.83	0.288

Gene	Fold change	p value
Lama2	1.67	0.360
Lama3	1.12	0.862
Lamb2	1.43	0.396
Lamb3	1.52	0.415
Lamc1	1.32	0.578
Mmp10	3.72	0.129
Mmp11	1.24	0.709
Mmp12	3.56	0.038
Mmp13	3.55	0.060
Mmp14	1.26	0.660
Mmp15	1.27	0.722
Mmp1a	4.23	0.056
Mmp2	1.28	0.499
Mmp3	7.69	0.009
Mmp7	2.26	0.203
Mmp8	1.62	0.180
Mmp9	1.61	0.303
Ncam1	2.82	0.067
Ncam2	2.01	0.227
Pecam1	2.00	0.046
Postn	2.61	0.183
Sele	2.30	0.239
Sell	4.72	0.005
Selp	3.90	0.062
Sgce	9.74	0.126
Sparc	3.08	0.388
Spock1	1.81	0.289
Spp1	1.23	0.611
Syt1	1.85	0.264
Tgfbi	0.49	0.082
Thbs1	2.65	0.070
Thbs2	5.82	0.067
Thbs3	2.97	0.017
Timp1	1.81	0.287
Timp2	0.69	0.419
Timp3	2.53	0.356
Tnc	0.58	0.605
Vcam1	1.86	0.280
Vtn	1.53	0.579
Gusb	1.12	0.579
Hprt1	0.58	0.530
Hsp90ab1	1.45	0.175
Gapdh	1.28	0.175
Actb	0.82	0.451